NATIONAL ENERGY TECHNOLOGY LABORATORY

Evaluating a Semi-Quantitative, Spectrophotometric Method for the Rapid Determination of Total Rare Earth Element Concentrations in Citrate Leaching Solutions

2 May 2023

U.S. DEPARTMENT OF ENERGY | NATIONAL ENERGY TECHNOLOGY LABORATORY

Office of Fossil Energy and Carbon Management

DOE/NETL-2023/4325

Disclaimer

This project was funded by the U.S. Department of Energy, National Energy Technology Laboratory, in part, through a site support contract.

Cover Illustration: Test tubes containing various amounts of calcium, iron, and lanthanum in the presence of the chromogenic reagent arsenazo(III).

Suggested Citation: Yang, J.; Bauer, S.; Verba, C. *Evaluating a Semi-Quantitative, Spectrophotometric Method for the Rapid Determination of Total Rare Earth Element Concentrations in Citrate Leaching Solutions*; DOE.NETL-2023.4325; NETL Technical Report Series; U.S. Department of Energy, National Energy Technology Laboratory: Albany, OR, 2023; p 24. DOI: https://doi.org/10.2172/1971983

An electronic version of this report can be found at:

https://netl.doe.gov/energy-analysis/search

Evaluating a Semi-Quantitative, Spectrophotometric Method for the Rapid Determination of Total Rare Earth Element Concentrations in Citrate Leaching Solutions

Jon Yang[1,2], Sophia Bauer[1,2], Circe Verba[1]

[1]National Energy Technology Laboratory, 1450 Queen Avenue SW, Albany, OR 97321, USA

[2]NETL Support Contractor, 1450 Queen Avenue SW, Albany, OR 97321, USA

DOE/NETL-2023/4325

2 May 2023

NETL Contacts:

Circe Verba, Principal Investigator

Burt Thomas, Technical Portfolio Lead

Bryan Morreale, Associate Laboratory Director for Research & Innovation, Research & Innovation Center

This page intentionally left blank.

Table of Contents

This page intentionally left blank.

List of Figures

List of Tables

Acronyms, Abbreviations, and Symbols

Term	Description
µM	Micromolar, micromoles per liter of solution
Arsz(III)	Arsenazo(III), a chromogenic indicator
Ca	Calcium
cm	Centimeters
HCl	Hydrochloric acid
ICP-MS	Inductively coupled plasma mass spectrometry
Fe	Iron
La	Lanthanum
Ln	14 naturally occurring lanthanide elements
M	Molar, moles per liter of solution
mL	Milliliters
NaOH	Sodium hydroxide
nm	Nanometers
REE	Rare earth elements: 14 naturally occurring lanthanides, Y, and Sc

Acknowledgments

This work was performed in support of the U.S. Department of Energy's (DOE) Fossil Energy and Carbon Management, Rare Earth Elements/Minerals Sustainability Field Work Proposal. The authors wish to thank Burt Thomas (Technical Portfolio Lead) for programmatic guidance, direction, and support.

ABSTRACT

Quick, reliable methods to measure the rare earth elements (REEs) in process streams are needed to support real-time parameterization and monitoring for a burgeoning number of REE extraction schemes. Such methods would ideally be fast, reproducible, and field-deployable. This study evaluates the feasibility of using a chromogenic indicator, arsenazo(III) (hereafter abbreviated as Arsz(III)) to detect the concentration of REEs in complex citrate leaching solutions using a spectrophotometer. Arsz(III) forms a chromogenic complex with the lanthanide elements that produces a blue/purple color detectable in the visible light range. Matrices of solutions containing varied concentrations of calcium, iron, and lanthanum were scanned in the presence of an Arsz(III) indicator to generate a modeled relationship that could be used to back calculate REE concentrations. While relatively quick (scan times on the order of seconds), the results indicated that the calcium and iron concentrations of typical mining solutions overwhelm the signal of the REEs, to the extent that sensitivity of the method is no less than 50 µM REEs. These results demonstrate the difficulties of accurately measuring trace metals in complex solutions, although the method may still hold utility for processes with significantly lower calcium and iron concentrations or REE concentrations much greater than 50 µM.

1. INTRODUCTION

With intensified interest in rare earth element (REE) extractions from various sources, there is a concomitant need to increase supporting peripheral activities such as the capability to rapidly and reliably assess the REE content of process streams. Such capabilities are important to adjust and inform real-time parameterization of a given process. For example, determining the duration of a reaction process can be set by specifying a cutoff value for REE concentrations, which could then be monitored in near real-time, thereby helping to balance operational costs.

Of the technical options available, spectrophotometric detection of the REEs in the visible light range offers a relatively cost-effective and rapid way to quickly scan process liquids for REE content. In the spectrophotometric method, a chromogenic reagent is added to a liquid sample which is then scanned through a spectrophotometer equipped with a simple white light source. The acquisition of the full absorbance spectra is typically a rapid operation (on the order of seconds) with most commercially available spectrometers. Such methods could even be field-deployable with enough foresight for sample preparation and the use of compact, portable spectrophotometric platforms. However, widespread adoption of a visible light spectrophotometric method is not commonplace in industry or academia due to some inherent technical challenges in the method, including the need for selective sensing materials in complex environments that are typically low pH and contain high concentrations of potentially interfering metals. In this study, we attempt to address some of these challenges to present a workable method for rapid REE detection within a constrained operational envelope.

One of the known technical challenges is the non-specificity of the chromogenic reagent selected for REE complexation and detection. To the authors' knowledge the only chromogenic reagent that has been utilized in isolated cases for REE determination is the arsenazo(III) compound (hereafter abbreviated as Arsz(III)). Arsz(III) is a synthetic dye containing arsenic acid functionalization that was originally synthesized as a chromogenic indicator for the actinide series (e.g., Savvin, 1961, 1969). Arsz(III) has seen applications for quantifying the levels of lanthanum (La) in biomedical media (e.g., Hogendoorn et al., 2018), REEs from phosphate mining wastes (e.g., Aly and Mohamed, 1999), actinides in waste streams (e.g. Pippin et al., 1984), and Ca in different media (e.g., Ohnishi et al., 1962; Ohnishi, 1979; Bauer, 1981). However, Arsz(III) is a non-selective complexant and will form complexes with most transition, alkali, and alkaline earth metals. This non-specificity in binding to metals leads to difficulties in isolating the REE-Arsz(III) complex signal in complex solutions where an abundance of other metals are present. The complexation of Arsz(III) with metal species is also highly sensitive to variations in pH (e.g., Rohwer et al., 1995; Rohwer and Hosten, 1997). In some cases, the pH value can be manipulated to increase the signal of a desired analyte while decreasing the interference from other matrix ions. For example, in biological media, mediating the pH between 2.8–3.0 maximized the signal of an Arsz(III)-La complex over an Arsz(III)-calcium(Ca) complex, where La concentrations were 0.1 to 10 µM and Ca concentrations up to 200 µM (Hogendoorn et al., 2018). Liquids such as those used in the leaching of underclays, however, present a much stiffer challenge, both from an increased loading of additional metals, and the orders of magnitude greater concentrations of interfering cations (e.g., Montross et al., 2020; Yang et al., 2022). Representative compositions of citrate leaching solutions from Montross et al. (2020) and Yang et al. (2022) were used as the basis for the development of spectrophotometric methods. In this experimental procedure, we attempt to elucidate the signals of Arsz(III)-metal complexes in complex citrate leaching solutions in the hopes of obtaining a clear signal of Arsz(III)-lanthanide (Ln) complexation. We employ a series of two- and three-phase testing matrices to reconstruct a model of REE quantification.

2. METHODS

Synthetic solutions were prepared in 0.1 M (molar) citrate matrices to match leaching solutions used in the citrate leaching of underclays (e.g., Montross et al., 2020; Yang et al., 2020). The pH was carefully adjusted using 1 M sodium hydroxide (NaOH) or 1 M hydrochloric acid (HCl) to a value of 2.8±0.05. The major cations found mobilized in the citrate leaching of underclays were dominantly Ca and Fe (presumed to be ferrous iron through the dissolution of Fe-sulfide minerals).

Solutions containing known concentrations of Ca, ferrous iron (Fe), La, and combinations thereof, were prepared from metal salts (Beantown Chemical). Ca concentrations were prepared from a range of 200 to 50,000 uM, Fe concentrations from 20 to 50,000 uM, and La concentrations from 2 to 100 uM, approximating concentrations observed in citrate leaching solutions after reaction with underclays (e.g., Montross et al., 2020; Yang et al., 2020). Individual calibration curves were run for each element before a series of binary matrices were run for Ca-Fe, Fe-La, and Ca-La, in the same concentration ranges.

Measurement of the absorbance spectra were conducted on 3 milliliters (mL) of each sample prepared in optical cuvettes with 1 centimeter (cm) path lengths. Arsenazo(III) solution was added to the cuvettes to a final concentration of 100 μM Arsz(III). The samples were scanned on a Vis-NIR spectrometer equipped with a tungsten halogen white light source (Ocean Insight Flame VIS-NIR) from 350 to 750 nanometers (nm).

Model fits were applied to the calibration curves of individual metal systems to find the best curvilinear fit. All model relationships were fit and parameterized using a least-squares method. These relationships formed the starting point to build model relationships in each of the binary systems (Ca-Fe, Fe-La, Ca-La). Following the binarization of the systems, the three-component system was modeled and fit based on the binary models. Finally, the three-component model was applied to experimental citrate leaching solutions and the degree of fit evaluated based on measured data through ICP-MS analyses (Yang et al., 2022).

3. RESULTS AND DISCUSSION

3.1 CALIBRATION CURVES

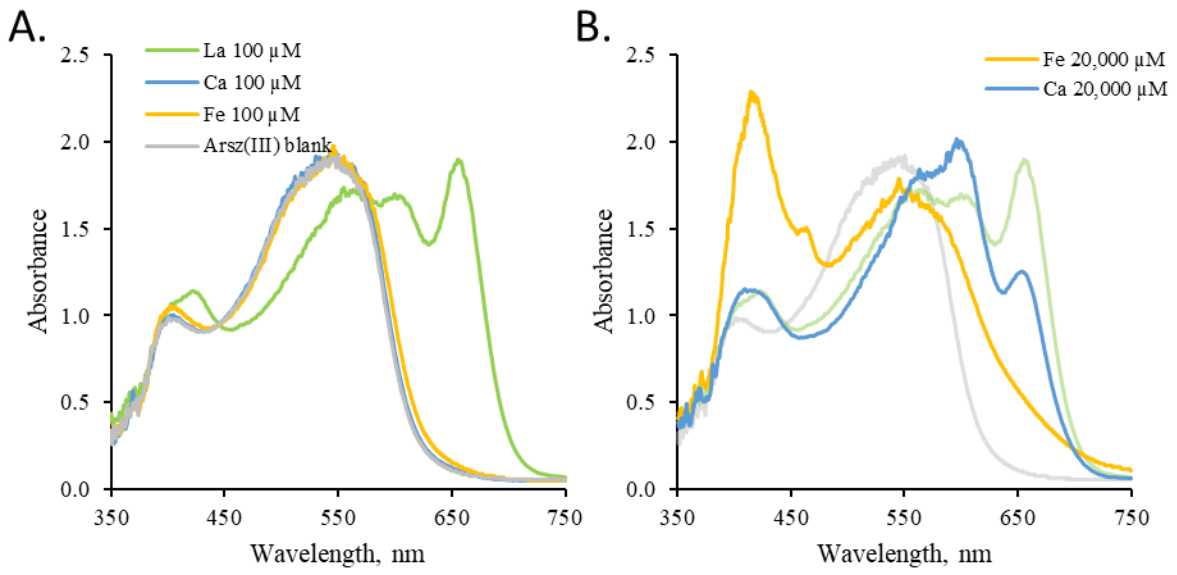

Figure 1: Full spectra absorbance scans of 100 µM Arsz(III) solutions with individual concentrations of A. 100 µM of La, Ca, or Fe, and B. 20,000 µM of Fe or Ca.

The absorbance peak for the La-Arsz(III) complex was determined at 660 nm (Figure 1), where La produced the most pronounced change in absorbance relative to Fe or Ca. The calibration curves for each element were subsequently determined at this wavelength (660 nm). Iron, however, did not have an absorbance peak in this wavelength region, but still displayed an increased response with increasing concentration (Figure 1B). The response of the absorbance peak at 660 nm with elemental concentration was determined to be non-linear for all elements tested. Calibration curves were fit to an exponential function (Eq. 1, Figure 2 via the least-squares method and individual calibration curve parameters reported in Table 1)

$$Abs660 = a - (a - b)\exp(-c[X]) \qquad \text{Eq. 1}$$

where *Abs660* is the absorbance value at 660 nm, a, b, and c are empirically derived constants, and *[X]* is the metal concentration (µM). This relationship is seen to hold generally true for the binary and ternary systems, with some added dependencies as discussed below.

Table 1: Individual Calibration Curve Parameters for Ca, Fe, La

	a	b	c	r^2
Ca	1.32	0.14	0	0.95
Fe	2.50	0.96	8.0E-05	0.99
La	2.28	0.09	1.7E-02	0.99

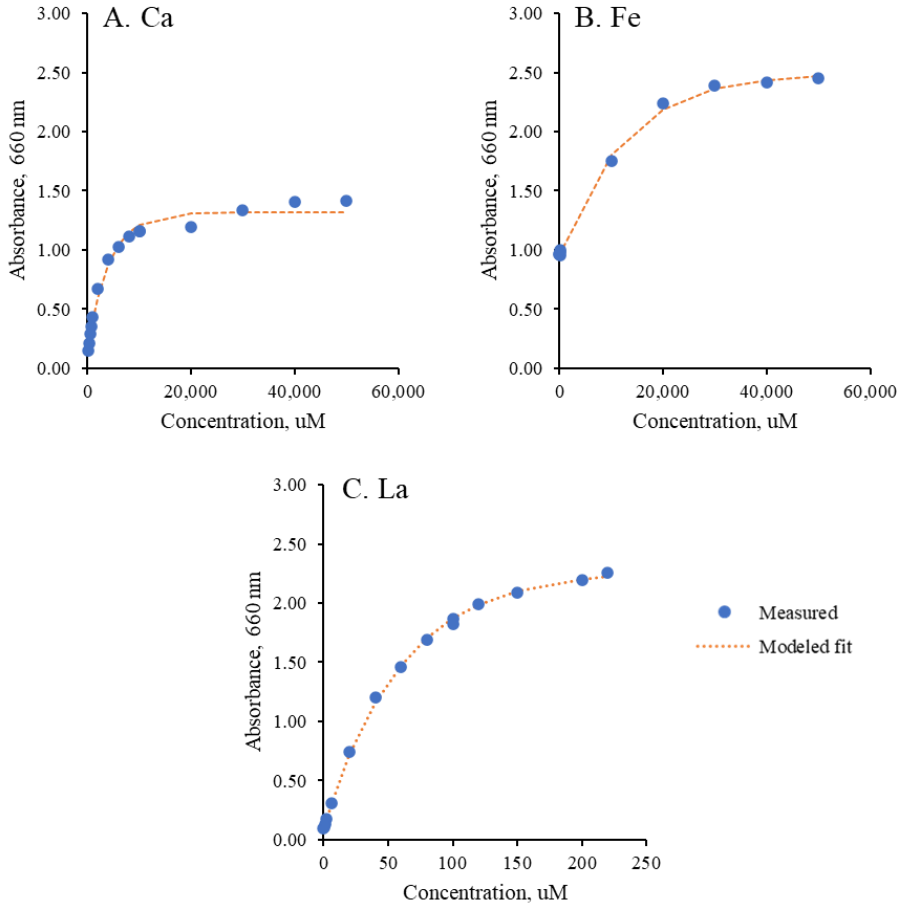

Figure 2: Calibration curves for absorbance at 660 nm wavelength for A. Ca, B. Fe, and C. La.

3.2 FE SUPPRESSION OF CA, LA ABSORBANCE PEAKS AT 660 NM WAVELENGTH

The combination of Fe and Ca in solution has the effect of suppressing the Ca-Arsz(III) absorbance peak at 660 nm (Figure 3A). This suppression effectively "flattens" the response of the absorbance signal to variations in Ca concentration. With progressive increases in Fe concentration, the slope of the Ca response curve gradually approaches a value of zero (Figure 3B). Over the range of Ca concentrations (200-50,000 µM) investigated, in the presence of Fe, the response curve is best fit to a linear relationship (Table 2).

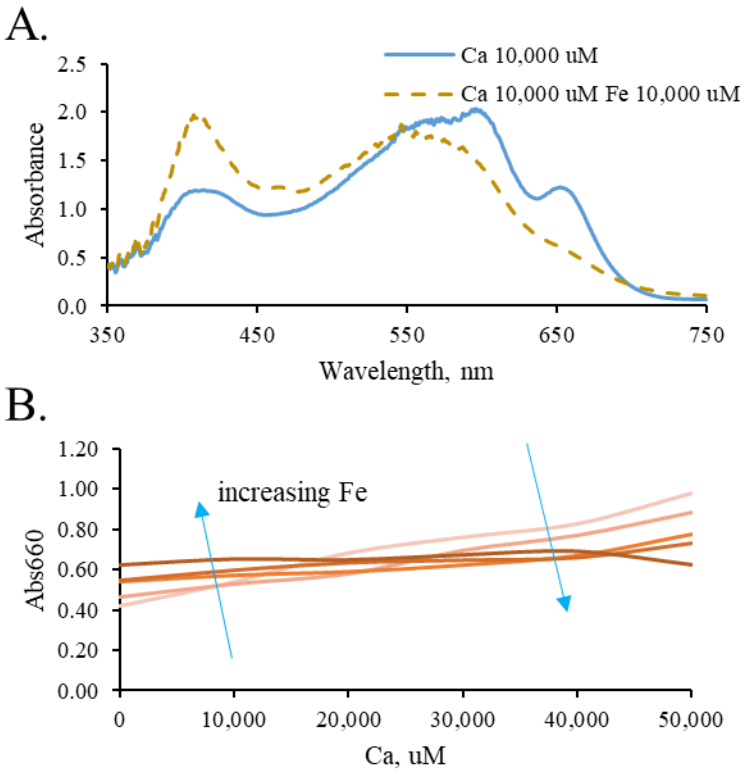

Figure 3: A. Full spectra scans of 10,000 µM Ca solutions with and without 10,000 µM Fe. B. Absorbance values at 660 nm wavelength as a function of increasing Ca and Fe concentrations.

Table 2: Modeled Parameters for Fitting the Binary Ca-Fe System as a Function of Abs660 and [Ca]

$Abs600_{CaFe}=m_{CaFe[Ca]}+b_{CaFe}$			
$m_{CaFe}=slope_1[Fe]+int_1$		$b_{CaFe}=slope_2[Fe]+int_2$	
$slope_1$	-2.61E-10	$slope_2$	5.45E-06
int_1	1.33E-05	int_2	3.50E-01

A consequence of the suppression of the absorbance signal at 660 nm is a concomitant increase in the model uncertainty with increasing Fe concentrations. The magnitude of the model uncertainty incorporates the relatively smaller contributions of the measurement uncertainty from the spectrophotometer (2-sigma < 0.06) and the uncertainty of the model regression to the measured data. Figure 4 illustrates the scale of the model uncertainty. Two representative cases are shown for the Ca concentrations ranging from 0 to 50,000 μM: one in the presence of 10,000 μM Fe and one in the presence of 40,000 μM Fe. At a given Ca concentration, the model uncertainty can be seen to be significantly larger in the 40,000 μM Fe case than in the 10,000 μM Fe case. For example, at a nominal concentration of 50,000 μM Ca, the model prediction using the 10,000 μM Fe case comes within 8% of the actual value with a total uncertainty of ±7% (2-sigma) (blue symbology in Figure 4).

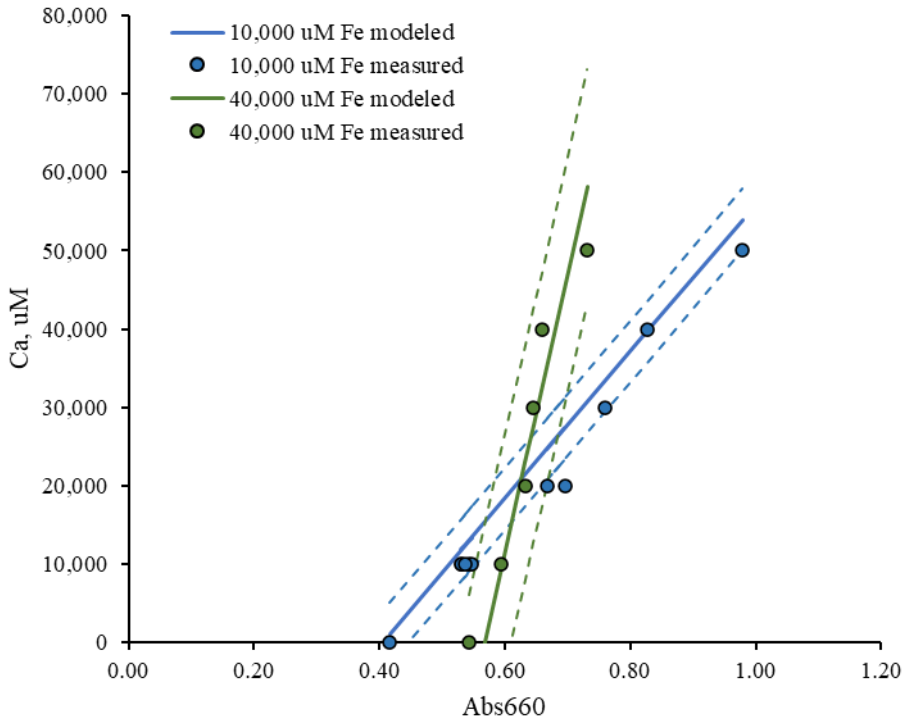

Figure 4: Modeled results for Ca concentrations from measured Abs660 values with the inclusion of 10,000 μM Fe (blue symbology) and 40,000 μM Fe (green symbology). Modeled results shown as solid lines with dashed lines indicating the uncertainty. Measured values are plotted as solid symbols.

Similarly, the suppression effect of Fe can be defined in the binary Fe-La system. With increasing Fe concentrations, the absorbance spectra response to the La-Arsz(III) complex gradually approaches a slope of zero (Figure 5). Practically, this results in increasing La concentrations having little to no effect on the measured Abs660 signal in the presence of abundant Fe. Nevertheless, the model fit to the data was found to best approximate Eq. 1 as discussed in Section 3.1 (Table 3).

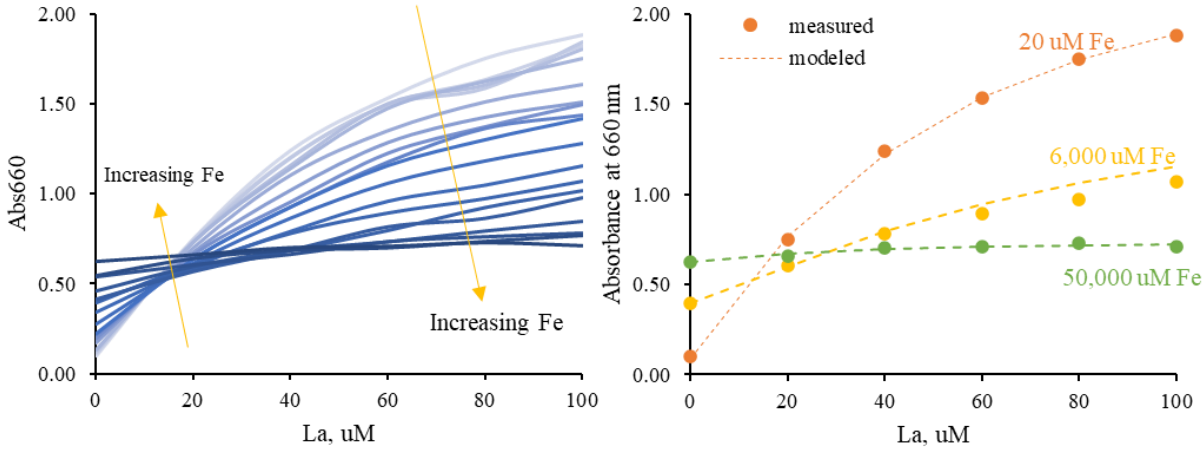

Figure 5: Effect of increasing Fe concentrations on the regressed curves for La at Abs660. A. Absorbance values at Abs660 as a function of increasing La and Fe concentrations. B. Discrete Fe concentrations at 20, 6,000, and 50,000 µM shown for the Abs660 response to increasing La concentrations.

Table 3: Modeled Parameters for Fitting the Binary Fe-La System as a Function of Abs660 and [La]

$Abs600_{FeLa}=A_{FeLa}-(A_{FeLa}-B_{FeLa})exp(-C_{FeLa}[La])$			
$A_{FeLa}=exp(-A_{FeLa,1}[Fe])+A_{FeLa,2}$		$B_{FeLa}=B_{FeLa,1}-(B_{FeLa,1}-B_{FeLa,2})exp(-B_{FeLa,3}[Fe])$	
$A_{FeLa,1}$	7.36E-04	$B_{FeLa,1}$	5.82E-01
$A_{FeLa,2}$	1.23E+00	$B_{FeLa,2}$	1.58E-01
$C_{FeLa}=C_{FeLa,1}exp(-C_{FeLa,2}[Fe])$		$B_{FeLa,3}$	1.17E-04
$C_{FeLa,1}$	1.69E-02		
$C_{FeLa,2}$	4.14E-05		

As in the binary system of Ca-Fe as well as in the binary Fe-La system, the model uncertainty increases with increasing concentrations of Fe. For the highest La signal measured at 100 µM, the model uncertainty increases from ~7% (2-sigma) at 20 µM concentrations of Fe to ~37% at the concentrations of 50,000 µM Fe (Figure 6).

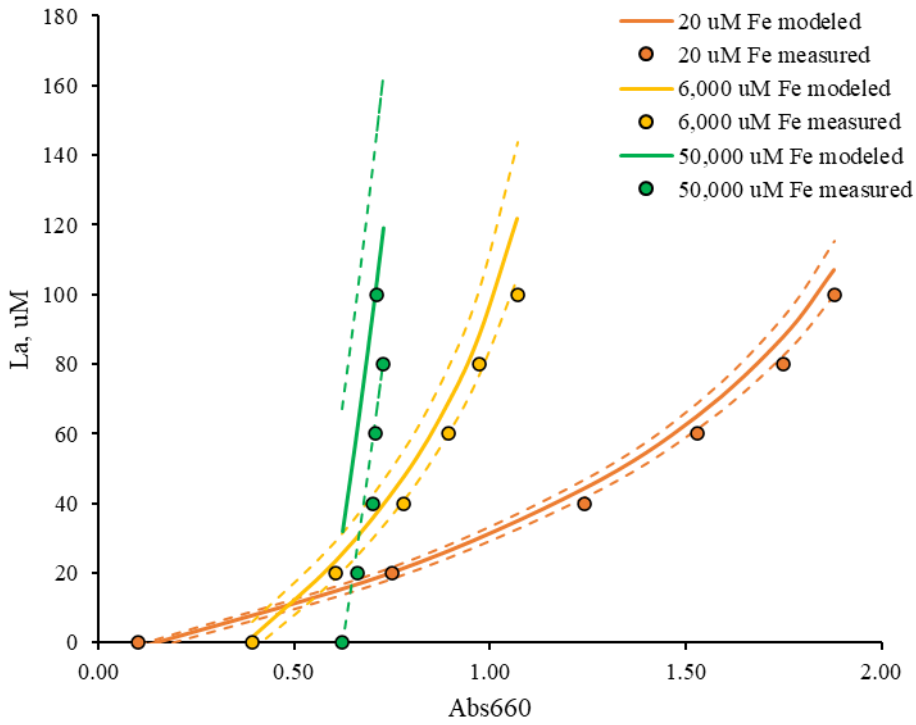

Figure 6: Modeled results for La concentrations from measured Abs660 values in the presence of 20 µM Fe (oranger symbology), 6,000 µM Fe (yellow symbology), and 50,000 µM Fe (green symbology). Modeled results shown as solid lines with dashed lines indicating the uncertainty. Measured values are plotted as solid symbols.

3.3 DECONVOLUTING CA FROM LA ABSORBANCE SIGNAL AT 660 NM WAVELENGTH

With the binary systems of Ca-Fe and Fe-La, the presence of Fe suppressed the absorbance signal at 660 nm for both the Ca- and La- Arsz(III) complexes. A similar effect is observed in the binary Ca-La system, with the added caveat that both the Ca- and La- Arsz(III) complexes express absorbance peaks at 660 nm wavelength (Figure 7). Nevertheless, suppression of the absorbance signal is observed with increasing concentrations of Ca. Eq. 1 is again parameterized to fit to the data (Table 4).

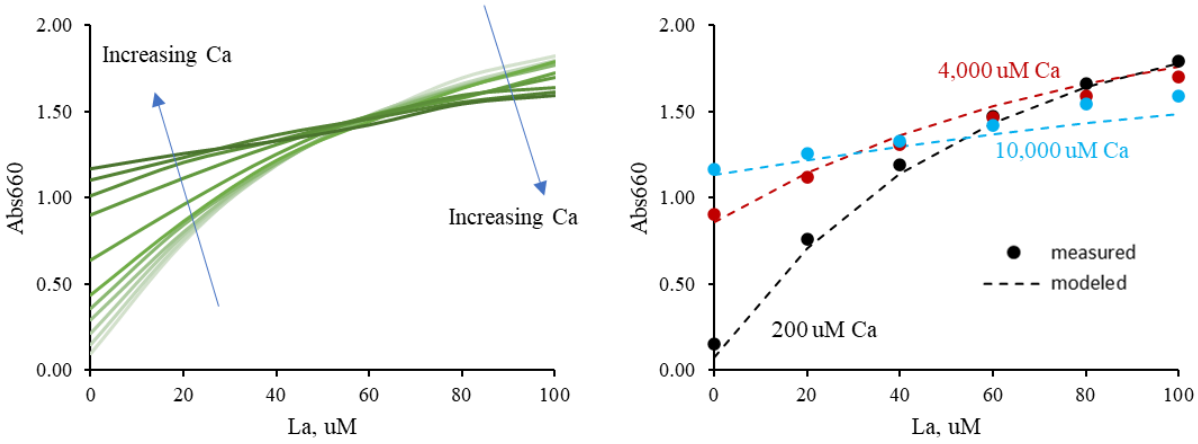

Figure 7: Effect of increasing calcium concentrations on the regressed calibration curves for La. A. Abs660 values as a function of increasing La and Fe concentrations. B. Discrete Fe concentrations at 200, 4,000, and 10,000 µM shown for the Abs660 response to increasing La concentrations.

Table 4: Modeled Parameters for Fitting the Binary Ca/La System as a Function of Abs660 and [La]

$Abs600_{CaLa}=A_{CaLa}-(A_{CaLa}-B_{CaLa})exp(-C_{CaLa}[La])$			
A_{CaLa}		$B_{CaLa}=B_{CaLa,1}-(B_{CaLa,1}-B_{CaLa,2})exp(-B_{CaLa,3}[Fe])$	
A_{CaLa}	2.08E+00	$B_{CaLa,1}$	1.18E+00
$C_{CaLa}=C_{CaLa,1}exp(-C_{CaLa,2}[Fe])$		$B_{CaLa,2}$	1.14E-03
$C_{CaLa,1}$	2.05E-02	$B_{CaLa,3}$	3.20E-04
$C_{CaLa,2}$	1.00E-04		

Compared to the binary Ca-Fe and Fe-La systems, the relative uncertainty of the model is lower for Ca/La, typically ranging from 8–12% (2-sigma) for a 100 µM concentration of La. The accuracy, however, of the model is shown to deviate significantly from the measured data, with the model overestimating the La concentration by as much as 40% (Figure 8).

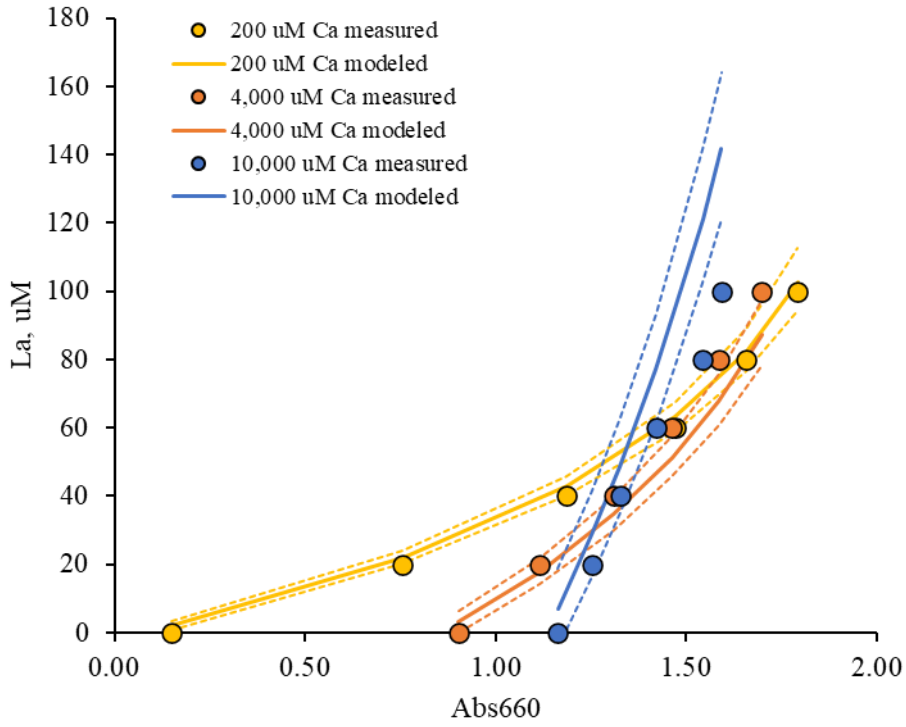

Figure 8: Modeled results for La concentrations from measured Abs660 values in the presence of 200 µM Ca (yellow symbology), 4,000 µM Ca (orange symbology), and 10,000 µM Ca (blue symbology). Modeled results shown as solid lines with dashed lines indicating the uncertainty. Measured values are plotted as solid symbols.

3.4 BUILDING A THREE-COMPONENT MODEL

With the parameterization of the three binary component systems (Ca-Fe, Fe-La, Ca-La), a three-component model can now be built and tested. In fitting a model to standardized solutions containing varying concentrations each of Ca, Fe, and La, a singular model framework was not suitable for the entire range of concentrations. Instead, the best fit to the measured data was found to be a conditional model where the binary Fe-La model is applied in conditions where [Fe] > 0 and the binary Ca/La model applied where [Fe] = 0 (Eq. 2).

$$Abs660 = \begin{cases} A_{FeLa} - (A_{FeLa} - B_{FeLa})\exp\left(-C_{FeLa}[La]\right), & [Fe] > 0 \\ A_{CaLa} - (A_{CaLa} - B_{CaLa})\exp\left(-C_{CaLa}[La]\right), & [Fe] = 0 \end{cases} \quad \text{(Eq. 2)}$$

This conditional switching of models was found to provide a reasonable degree of agreement between measured and modeled absorbance values at 660 nm wavelength (Figure 9).

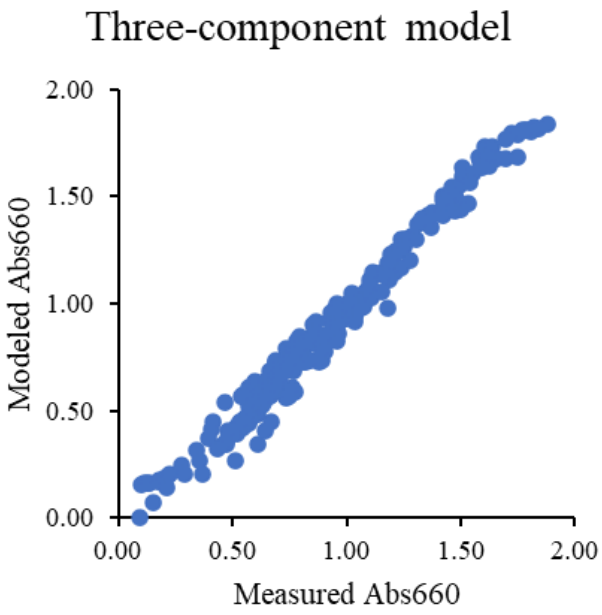

Figure 9: Three-component model comparison of modeled Abs660 values to measured values.

3.5 MODEL TESTS ON EXPERIMENTAL SOLUTIONS

In reality, most experimental solutions involved in the leaching of geologic materials will contain dissolved iron in some amount—thus, the Fe-La model will be the most appropriate model to apply. Leachate solutions from experimental extractions using citric acid on coal seam underclays were scanned using the Arsz(III) method, and the Fe-La model applied. In this case, an important distinction in the method is that Fe, Ca, and La (as well as a suite of other geochemical data) were measured via inductively coupled plasma mass spectrometry (ICP-MS) from previous work (Yang et al., 2022). The Fe-La model could then easily be applied using the known values for Fe and comparing the results for the modeled La versus the measured total lanthanide concentration (Ln, representing the sum of the lanthanide element concentrations) (Figure 10).

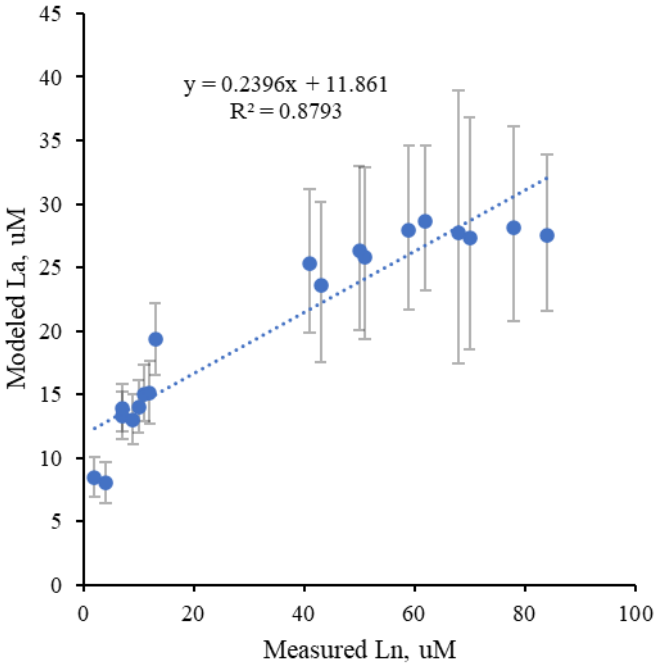

Figure 10: Modeled La concentrations plotted against measured Ln concentrations in the experimental citrate leachates. Ln concentrations denote the sum of the 14 naturally occurring lanthanide elements. Analytical error in the measured Ln values are between 2-5% and are smaller than the marker shown.

The modeled La concentrations can be seen to fall short of the measured Ln concentration in the experimental solutions with wide lower and upper uncertainty limits, although a linear trend can generally describe the relationship (Figure 10). A mismatch between the modeled La and measured Ln signals were expected, however, as the La-Arsz(III) complex is not the only signal of Ln-Arsz(III) complexation in these experimental solutions. Indeed, the La-Arsz(III) complex was assumed to be an appropriate choice of a proxy measurement to approximate the total lanthanide concentration in solution.

Using the linear regression parameters between modeled La and measured Ln (Figure 10), an estimated modeled value of Ln can be derived (Figure 11). The values returned from this combination of modeling are in reasonable agreement with the measured results, but the uncertainties surrounding the modeled values are large. The propagated uncertainties in the modeled values can range as high as 33% (2-sigma) of the indicated value. Practically, these results indicate that the model can detect large deviations in Ln concentrations greater than ~50 µM, but would have difficultly distinguishing any variation smaller than 50 µM.

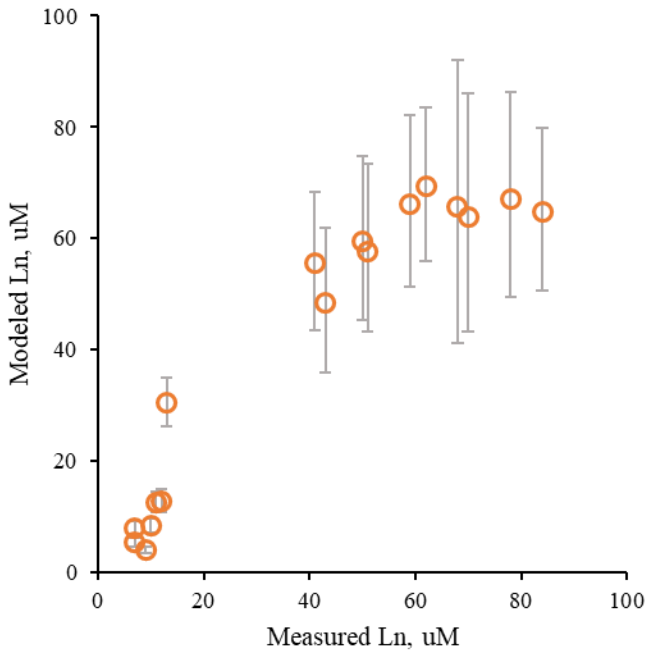

Figure 11: Modeled Ln concentrations after applying a linear correction plotted against measured Ln concentrations. Analytical error in the measured Ln values are between 2-5% and are smaller than the marker shown.

4. CONCLUSIONS

A spectrophotometric method for REE determination in complex mining solutions using arsenazo(III) shows some limited utility to estimate concentrations in a semi-quantitative manner. Interferences from Fe and Ca, two common metals encountered in complex mining solutions, in solution mask the signal of the Ln-Arsz(III) to the degree where the sensitivity of the method is limited to > 50 µM Ln (~7 mg/L). Practically, this sensitivity means that this spectrophotometric method is only suitable for rather large excursions in dissolved Ln concentrations. For example, in the experimental solutions tested using this spectrophotometric method, the sample-to-sample variability in measured Ln concentration never deviated by more than 40 µM, leading to the high uncertainty presented in Figure 11. Ultimately this spectrophotometric method may prove useful, but only in monitoring processes with sufficiently large swings in Ln concentrations or with greatly reduced concentrations of Ca and Fe.

Other limitations of this spectrophotometric method should also be acknowledged to objectively evaluate the applications of the method. The testing regimen presented within this study is predicated on the pre-existing knowledge of the concentration of Fe and Ca present in solution. In reality, of course, these values would be unknown for freshly generated samples of mining solutions. These concentrations would have to be first determined before the model can be applied. Fortunately, spectrophotometric methods exist for the determination of both Fe and Ca in solution (e.g., Harvey et al., 1955; Bauer, 1981), but additional runtime and uncertainty will be added. Dissolved Fe in solution can be read at 510 nm using a 1,10-phenanthroline indicator with a working range from 0.1 to 300 mg/L (Harvey et al., 1955). Dissolved Ca can be measured using the Arsz(III) reagent at a relatively high dilution level. Once Fe and Ca concentrations are determined, REE concentration may then be scanned at a lower dilution level.

Bearing in mind these unexpected barriers to implementation, the semi-quantitative estimation of dissolved REEs in complex solutions may be determined using a relatively simplistic spectrophotometric method. This method is constrained to cases with large concentrations and variations in signal of the REEs of >50 µM and/or when no significant Ca or Fe are present in solution. While relatively rapid, the method still requires sample preparation time and multiple readings to determine Fe and Ca concentrations first. Any deployment considerations to the field need to be carefully planned to ensure availability of reagents, equipment, and pH readings.

5. REFERENCES

Aly, M. M.; Mohammed, N. A. Recovery of lanthanides from Abu Tartur phosphate rock, Egypt. *Hydrometallurgy* **1999,** *52*, 199–206. https://doi.org/10.1016/S0304-386X(99)00018-3

Bauer, P. J. Affinity and stoichiometry of calcium binding by arsenazo III. *Analytical Biochemistry* **1981,** *110*, 61–72. https://doi.org/10.1016/0003-2697(81)90112-3

Harvey, A. E.; Smart, J. A.; Amis, E. S. Simultaneous Spectrophotometric Determination of Iron(ll) and Total Iron with 1,10-Phenanthroline. *Analytical Chemistry* **1955,** *27*, 26–29. https://doi.org/10.1021/AC60097A009/ASSET/AC60097A009.FP.PNG_V03

Hogendoorn, C.; Roszczenko-Jasińska, P.; Martinez-Gomez, N. C.; de Graaff, J.; Grassl, P.; Pol, A.; Op den Camp, H. J. M.; Daumann, L. J. Facile Arsenazo III-based assay for monitoring rare earth element depletion from cultivation media for methanotrophic and methylotrophic bacteria. *Applied and Environmental Microbiology* **2018,** *84*. https://doi.org/10.1128/AEM.02887-17

Montross, S. N.; Yang, J.; Britton, J.; McKoy, M.; Verba, C. Leaching of Rare Earth Elements from Central Appalachian Coal Seam Underclays. *Minerals* **2020,** *10*, 577. https://doi.org/10.3390/MIN10060577

Ohnishi, T. S. A method of estimating the amount of calcium bound to the metallochromic indicator arsenazo III. *Biochimica et Biophysica Acta (BBA) - General Subjects* **1979,** *586*, 217–230. https://doi.org/10.1016/0304-4165(79)90094-1

Onishi, H.; Nagai, H.; Toita, Y. Spectrophotometric determination of rare earth elements and thorium with arsenazo. *Analytica Chimica Acta* **1962,** *26*, 528–531. https://doi.org/10.1016/S0003-2670(00)88426-3

Rohwer, H.; Collier, N.; Hosten, E. Spectrophotometric study of arsenazo III and its interactions with lanthanides. *Analytica Chimica Acta* **1995,** *314*, 219–223. https://doi.org/10.1016/0003-2670(95)00279-9

Rohwer, H.; Hosten, E. pH dependence of the reactions of arsenazo III with the lanthanides. *Analytica Chimica Acta* **1997,** *339*, 271–277. https://doi.org/10.1016/S0003-2670(96)00471-0

Savvin, S. B.; Propistsova, R. F.; Strel'nikova, R. v. ARSENAZO M: A NEW REAGENT FOR THE RARE EARTH ELEMENTS. *Zh. Anal. Khim.* **1969,** *24*, *31-8(Jan. 1969)*, 673–685. https://doi.org/10.1016/0039-9140(61)80164-1

Savvin, S. B. Analytical use of arsenazo III. Determination of thorium, zirconium, uranium and rare earth elements. *Talanta* **1961,** *8*, 673–685. https://doi.org/10.1016/0039-9140(61)80164-1

Yang, J.; Montross, S.; Britton, J.; Stuckman, M.; Lopano, C.; Verba, C. Microanalytical Approaches to Characterizing REE in Appalachian Basin Underclays. *Minerals* **2020,** *10*, 546. https://doi.org/10.3390/min10060546

Yang, J.; Bauer, S.; Verba, C. *Strategies to Recover Easily-Extractable Rare Earth Elements and Other Critical Metals from Coal Waste Streams and Adjacent Rock Strata Using Citric Acid*; DOE.NETL-2022.3732; NETL Technical Report Series; U.S. Department of Energy, National Energy Technology Laboratory: Albany, OR, 2022; p. 28. DOI: 10.2172/1884275

Brian J. Anderson
Director
National Energy Technology Laboratory
U.S. Department of Energy

Jessica Mullen
Federal Technology Manager
Rare-Earth Elements & Critical Minerals
National Energy Technology Laboratory
U.S. Department of Energy

Anna Wendt
Program Manager
Minerals Sustainability
U.S. Department of Energy

Bryan Morreale
Associate Laboratory Director for Research & Innovation
Research & Innovation Center
National Energy Technology Laboratory
U.S. Department of Energy

R. Burt Thomas
Technical Portfolio Lead
Critical Minerals
National Energy Technology Laboratory
U.S. Department of Energy

NETL Technical Report Series